Brain Behav Immun. Author manuscript; available in PMC 2010 July 01.

Published in final edited form as:
Brain Behav Immun. 2009 October ; 23(7): 1003–1013. doi:10.1016/j.bbi.2009.05.061.

Disturbed distribution of proliferative brain cells during lupus-like disease

Mile Stanojcic[1], **Tal Burstyn-Cohen**[2], **Nadia Nashi**[2], **Greg Lemke**[2], and **Boris Sakic**[1]

[1] Department of Psychiatry and Behavioural Neurosciences, McMaster University and The Brain-Body Institute, St. Joseph's Healthcare Hamilton, Ontario, CANADA

[2] The Salk Institute, San Diego, USA

Abstract

Brain atrophy and neuronal degeneration of unknown etiology are frequent and severe concomitants of the systemic autoimmune disease lupus erythematosus (SLE). Using the murine MRL/lpr model, we examined populations of proliferative brain cells during the development of SLE-like disease and brain atrophy. The disease onset was associated with reduced expression of Ki67 and BrdU proliferation markers in the dorsal part of the rostral migratory stream, enhanced Fluoro Jade C staining in the subgranular zone of the dentate gyrus, and paradoxical increase in density of $Ki67^{+}/BrdU^{-}$ cells in the paraventricular nucleus. Protuberances containing clusters of $BrdU^{+}$ cells were frequent along the lateral ventricles and in some cases were bridging ventricular walls. Cells infiltrating the choroid plexus were $Ki67^{+}/BrdU^{+}$, suggesting proliferative leukocytosis in this cerebrospinal fluid-producing organ. The above results further support the hypothesis that systemic autoimmune disease induces complex CNS pathology, including impaired neurogenesis in the hippocampus. Moreover, changes in the paraventricular nucleus implicate a metabolic dysfunction in the hypothalamus-pituitary-adrenal axis, which may account for altered hormonal status and psychiatric manifestations in SLE.

Keywords

Lupus; Brain cell proliferation; Hippocampus; Neurogenesis; Autoimmunity; Brain atrophy; MRL model

Introduction

Systemic autoimmune disease lupus erythematosus (SLE) is frequently accompanied by neurologic and psychiatric complications (Bosma, Middelkoop, Rood, Bollen, Huizinga, and van Buchem, 2002). Brain imaging reveals lesions in the periventricular and subcortical white matter (Jennings, Sundgren, Attwood, McCune, and Maly, 2004), hypoperfusion (Handa, Sahota, Kumar, Jagannathan, Bal, Gulati, Tripathi, and Wali, 2003), and regional

Correspondence: Boris Sakic, Ph.D. Associate Professor, Department of Psychiatry and Behavioral Neurosciences, McMaster University, The Brain-Body Institute, St. Joseph's Healthcare, Juravinski Innovation Center T-3307, Ontario, Canada L8N 4A6, tel.: (905) 522-1155 ext. 35220, fax: (905)-540-6593, sakic@mcmaster.ca.
Note: Mile Stanojcic and Tal Burstyn-Cohen had contributed equally to study and share first authorship.

metabolic abnormalities (Appenzeller, Costallat, Li, and Cendes, 2006). The damaged blood-brain barrier (Abbott, Mendonca, and Dolman, 2003), brain atrophy, and ventricular enlargement (Kozora, West, Kotzin, Julian, Porter, and Bigler, 1998; Waterloo, Omdal, Jacobsen, Klow, Husby, Torbergsen, and Mellgren, 1999) further suggest that SLE progression induces a widespread neuronal loss by unknown pathogenic mechanisms (Sibbitt, Haseler, Griffey, Hart, Sibbitt, and Matwiyoff, 1994).

Inbred MRL/MpJ-Fas^{lpr} (MRL/lpr) mice develop an accelerated form of SLE-like disease due to insertional inactivation of the Fas receptor gene (Watanabe-Fukunaga, Brannan, Copeland, Jenkins, and Nagata, 1992). Compared to congenic MRL/MpJ (MRL +/+) controls that develop the disease later, the onset of autoimmunity in MRL/lpr mice is accompanied by an anxious/depressive-like behavioral profile (Sakic, Szechtman, Talangbayan, Denburg, Carbotte, and Denburg, 1994), ventricular enlargement (Denenberg, Sherman, Rosen, Morrison, Behan, and Galaburda, 1992), cerebral atrophy, retarded brain growth (Sakic, Szechtman, Denburg, Gorny, Kolb, and Whishaw, 1998), and infiltration of immunocompetent cells into the choroid plexus (James, Hutchinson, Bullard, and Hickey, 2006) and brain parenchyma (Ma, Foster, and Sakic, 2006). Several lines of evidence suggest that neuronal viability is compromised in the subventricular zone (SVZ) of lateral ventricles and the subgranular zone (SGZ) of the dentate gyrus, which are the main neurogenic regions in the adult mammalian brain (Martino and Pluchino, 2006). Areas around the lateral ventricles show enhanced neurodegeneration, as revealed by Fluoro Jade B staining (Ballok, Millward, and Sakic, 2003) and excessive DNA fragmentation (Sakic, Maric, Koeberle, Millward, Szechtman, Maric, and Denburg, 2000). Hippocampal neurons show neurodegenerative changes at both dendritic and somatic levels (Sakic et al., 1998), while accumulations of basophilic cells are common in the SGZ (Ballok, Ma, Denburg, Arsenault, and Sakic, 2006).

One possibility is that the autoimmune process reduces the viability of both young and mature neurons. This lack of selectivity was shown in studies where autoimmune CSF was cytotoxic to a C17.2 neural stem cell line, neurospheres from MRL/lpr and healthy strain of mice, rat retinal neurons (Sakic, Kirkham, Ballok, Mwanjewe, Fearon, Macri, Yu, Sidor, Denburg, Szechtman, Lau, Ball, and Doering, 2005b), and neurons in primary hippocampal co-culture (Maric, Millward, Ballok, Szechtman, Barker, Denburg, and Sakic, 2001). Consistent with the notion of neurotoxic immunoglobulins (DeGiorgio, Konstantinov, Lee, Hardin, Volpe, and Diamond, 2001), MRL mice produce antibodies to the general cell proliferation marker Ki67 (Bloch, Rabkina, and Bloch, 1995; Scholzen and Gerdes, 2000). Conversely, one may expect that hyperbasophilic cells in the SGZ (Ballok et al., 2006) reflect a reparative mechanism triggered in response to hippocampal injury (Darsalia, Heldmann, Lindvall, and Kokaia, 2005; Danilov, Covacu, Moe, Langmoen, Johansson, Olsson, and Brundin, 2006). Taken together, the above evidence led to an expectation of significant changes in the major neurogenic regions at the onset of SLE-like disease. A recent study reported increased proliferative activity in SVZ of adult MRL +/+ mice (Baker, Daniels, Lennington, Lardaro, Czap, Notti, Cooper, Isacson, Frasca S Jr, and Conover, 2006). Given that MRL +/+ and MRL/lpr mice share more than 99.9% of their genome (Theofilopoulos, 1992), the comparison of their germinal centers can provide insight into how systemic autoimmunity affects the reparative capacity of the brain during the

progression of systemic inflammation and autoimmunity. For this purpose, we compared the distribution, phenotype, and density of proliferating cells during the development of SLE-associated brain atrophy.

Materials and Methods

Animals

Twenty-five four week old MRL/MpJ-*Fas*^{lpr}/2J (MRL-lpr; stock 6825) and twenty MRL/MpJ male mice (MRL+/+, stock 486) were purchased from the Jackson Laboratories (Bar Harbour, ME) and tail-tattooed for identification purposes (AIMS Inc, Hornell, NY). The MRL/lpr substrain (originally stock 485) was renamed as stock 6825 in 2007 because of a gradual loss of autoimmune phenotype over the past several years. In comparison to the original stock 485, mice from the stock 6825 develop milder autoimmune symptoms and live longer (http://jaxmice.jax.org/strain/006825.html). Despite this decline in phenotype, stock 6825 still develops serological manifestations of lupus-like disease earlier than mice from the MRL +/+ substrain. Neither overt manifestations (e.g. dermatitis, alopecia, lymphadenopathy), nor premature deaths were seen in the present study. Animals were housed under standard laboratory conditions (reversed lighting 8 P.M.–8 A.M.; food and water *ad libitum*) in groups of 4–5 per cage. At 4 months of age, all mice were injected with 5-bromo-2-deoxyuridine (BrdU; i.p. 50 μg/g body weight; Sigma) dissolved in 0.9% NaCl and sterile-filtered at 22 μm. Six injections were given at 24-h intervals. Twenty-four hours after the last injection, 10 mice per group were sacrificed and brains processed for immunohistochemical analysis, as described below. One month after the last BrdU injection, the second cohort of mice (15 MRL/lpr and 10 MRL +/+) were processed identically. When significant differences were observed in aged groups, 1-month-old MRL mice of both substrains (N = 8) and three 5-month-old, non-autoimmune C57Bl/6 mice were employed as healthy controls. The rationale for adding these groups was to determine whether changes in the brain were a consequence of dissimilar genetic background, aging, or autoimmunity. Given that splenomegaly is a hallmark of lupus-like disease in MRL mice (Theofilopoulos, 1992), wet spleen weight was measured upon extraction using an analytical scale. Similarly, brains were weighed immediately upon extraction. All experimental protocols were approved and carried out in accordance with the rules and regulations of the Salk Institute animal care committee.

Immunohistochemistry

At the end of the experiment, the mice were anesthetized with 2.5% Avertin in PBS (i.p., 0.4 mg/g body weight) and, after terminal bleeding from the heart, were intracardially perfused with saline, followed by ~120 ml of 4% paraformaldehyde (PFA in phosphate buffer) over 5 min. Brains were stored in fixative overnight and transferred into 30% sucrose before further processing. Frozen sections (40 μm thick) were cut coronally on a sliding microtome and stored at −20°C in a cryoprotectant containing 25% ethylene glycol, 25% glycerin in 0.05 M phosphate buffer. Proliferative cells were assessed by immunohistochemistry to BrdU (marker of S-phase) and general proliferation marker Ki67. NeuN is a nuclear protein antigen that is considered to be a marker for post-mitotic neurons in a given germinal zone. Primary and secondary antibodies were diluted in Tris-buffered saline containing 0.1%

Triton X-100 and 3% horse or donkey serum (TBS-plus). For BrdU immunohistochemistry, sections were incubated in 50% formamide/50% 2X SSC buffer (0.3 M NaCl/0.03 M sodium citrate) at 65°C for 2 h, rinsed twice in SSC buffer, incubated in 2 M HCl for 30 min at 37°C, and rinsed in 0.1 M borate buffer pH 8.5 for 10 min. Immunostaining for BrdU and NeuN was done as described previously (Kempermann, Kuhn, and Gage, 1997). The following antibodies were used: rat anti-BrdU ascites (1:200, Accurate, Harlan Sera-Lab, UK), mouse anti-NeuN (1:200, Chemicon, CA), rabbit anti-Ki67 (1:500, Vector labs, CA), rat anti-mouse CD3 (1:50, Serotec, UK), goat anti-DCX (1:100, Santa Cruz, CA), rabbit anti-GFAP (1:500, Dako, CA), donkey anti-rat FITC (1:250, Jackson ImmunoResearch, PA), donkey anti-mouse Cy3 (1:250, Jackson ImmunoResearch, PA), donkey anti-goat Cy3 (1:250, Jackson ImmunoResearch, PA), and donkey anti-rabbit AMCA (1:250, Jackson ImmunoResearch, PA). Cell counts and areas were assessed in a 1-in-6 series of coronal sections (240 μm apart) throughout the rostro-caudal extent. Areas of interest included choroid plexus, SVZ, and SGZ. However, an unexpected signal in the hypothalamic paraventricular nucleus (PVN) led to a detailed analysis of this region as well. To assess NeuN-BrdU double-labeled cells, a 1-in-12 series of sections was immuno-stained and analyzed by confocal microscopy (Zeiss, Bio-Rad, CA). One hundred BrdU-positive cells per dentate gyrus of 5-month-old MRL mice were analyzed for co-expression of BrdU and NeuN for neuronal phenotype, and ratios of cells co-expressing BrdU and NeuN were determined.

We used Stereo Investigator 5.05 package (MicroBright Field, Williston, VT) in the initial counting of proliferative cells in the DG. However, as shown on Figure 6B, the $BrdU^+$ cells were scarce in both groups of MRL mice and many counting frames had 0 counts. This observation was consistent with the 60–75% reduction in $BrdU^+$ cells in DG of MRL/MpJ (+/+ mice) in comparison to non-autoimmune C57BL/6 mice (Thuret, Toni, Aigner, Yeo, and Gage, 2009). Consequently, the required criterion of 2–5 cell count per counting frame could not be met and the Gundersen's coefficient of error was well above 15%. Conversely, it was difficult to define a sampling grid in the periventricular region because proliferating cells in the RMS of MRL-lpr were scattered in patches of irregular shape. Therefore, we employed AxioVision 4.6 software package (Zeiss USA) and Interactive Measurement plug-in to consistently quantify the signals in both zones. Frequency (cell count), signal area (per standard counting frame), and spline distance were used as adequate parameters.

Planimetric analysis

Brain sections were analyzed from +1.42 mm to −2.80 mm with respect to Bregma. Images of the lateral ventricles, SVZ, and hippocampus were digitized using Axioskop 2 Plus microscope (Carl Zeiss, Inc., CA), a 1X objective, and permanently mounted 0.63X lens adapter. The areas were outlined using a digital stylus (Intuos^3, Wacom, WA) and AxioVision 4.6 software package (Carl Zeiss Inc., CA). Six adjacent regions were assessed: +1.42 mm to +0.74 mm, +0.62 mm to +0.14 mm, +0.02 mm to −0.70 mm, −0.82 mm to −1.34 mm, −1.58 mm to −2.18 mm, and −2.30 mm to −2.80 mm. Brain atrophy was assessed as the ratio between the sum of lateral ventricle areas and brain area of the section inspected. A minimum of 4 digital images of the SGZ (ranging from −1.22 mm to −2.80 mm, relative to Bregma) were taken under a 10X objective and traced as described above.

Depending on the section, the length was defined as the distance from the dorso-lateral end of the lower blade to its sagittal endpoint or to the ventro-lateral end of the upper blade. $BrdU^+$ cells within the SGZ of both hemispheres were counted using a 20X objective.

The rostral migratory stream (RMS) was operationally defined as a projection of $BrdU^+$ and/or $Ki67^+$ cells between +1.42 mm and +0.74 mm from Bregma. The RMS was measured using fluorescent $Ki67^+$ sections in all ages and $BrdU^+$ sections from 4- and 5-month-old groups. A minimum of four planes, ranging from +1.42 mm to +0.74 mm, were examined using a 10X objective and AxioVision 4.6. The diameter was measured as the distance between the superior-lateral horn (proximal side) of the lateral ventricle and the furthest cluster of $BrdU^+$ cells at the distal part of the RMS on a given coronal section. In addition, the areas of $BrdU^+$ and $Ki67^+$ cells along the RMS and $Ki67^+$ cells in the PVN (−0.22mm to −1.06) were assessed using the Axiovision 4.6 and Interactive Measurement plug-in and counting frames 500μm × 500μm and 450μm × 450μm, respectively. Lateral ventricle protuberant nests (protuberances) in aged MRL mice were counted in both hemispheres. When fusion was observed, facing nests were counted as two protuberances.

Assessment of neurodegeneration

Fluoro Jade C stains (FJC: Histo-Chem, Inc.) degenerating neurons, regardless of specific insult or mechanism of cell death (Schmued, Stowers, Scallet, and Xu, 2005). It can be effectively used in localizing degenerating nerve cell bodies, distal dendrites, axons, and terminals. The staining was performed on a series of hippocampal sections from 5 mice per group according to manufacturer's instruction and as described earlier (Ballok et al., 2003). The FJC^+ cells in the hippocampus of 4- and 5-month-old mice were scored as follows: 0 = no FJC^+ cells; 1 = single scattered cells (~ <5%); 2 = a few clustered cells (~5–10%); 3 = clustered cells in several restricted regions (~10–50%); 4 = many cells in clusters (estimated as 50–80%); 5 = whole SGZ areas filled with FJC^+ cells (estimated as >80%). Since scanning through the SVZ revealed no FJC^+ cells, this region was not considered for subsequent analysis.

Statistical analysis

The data were analyzed by ANOVA with Substrain (MRL/lpr vs. MRL +/+) and Age (younger vs. older cohort) as between-group factors. When measures were taken repeatedly, ANOVA with repeated measures was used. Bonferroni's test was used in the post-hoc analysis. Pearson and Spearman correlations were used to measure association between variables. All computations were performed using the SPSS 13 statistical package. Graphs show mean values ± SEM, and significant differences of $p \leq .05$, $p < .01$ and $p < .001$ are indicated by *, **, and ***, respectively.

Results

Body weight and organ weight

In 4-month-old mice, body weight was lower in the MRL/lpr group than in the MRL +/+ group (41.2±1.4g in MRL/lpr vs. 45.9±0.47g in the MRL +/+ substrain; $|t_{18}|=3.105$, p=.006). As observed earlier (Sakic *et al.*, 1998; Sakic *et al.*, 2005b), increased spleen mass

(0.154±0.011g in MRL/lpr vs. 0.102±0.007g in MRL +/+ substrain; t_{18}=3.605, p=.002) and reduced brain weight (0.454±0.007g vs. 0.492±0.003g; substrain: $|t_{18}|$=3.605, p=.002) confirmed the autoimmune status and suggested brain atrophy in the MRL/lpr group. However, due to the positive correlation between brain and body weight (r_{51} = .746, p < .001), reduced brain weight in MRL-lpr mice was not deemed a representative measure of CNS atrophy. Given that ventricular enlargement is well documented in MRL/lpr mice (Denenberg *et al.*, 1992; Sakic, Hanna, and Millward, 2005a), the ratio between lateral ventricles and their respective brain area was used as a more reliable index of brain atrophy throughout the study.

Ventricles

The overall analysis across the ages revealed that the 5-month-old MRL/lpr mice showed increased ventricle/brain area ratio (Substrain: F(1,16) = 14.49, p = .002; Fig. 1A), which was not apparent in the younger groups. However, less conservative analysis with multiple T-tests revealed a significant single-section range difference that became more profound with advancing age and disease severity (1 month, Section 2: t_6 = 2.949, p = .026; 4 months, Section 4: t_{18} = 3.808, p = .001). This enlargement appears to be shifting from the SVZ region (illustrated on Figure 1B) towards the hippocampus, ultimately encompassing a larger area when the disease is fully developed in the MRL/lpr substrain.

The lateral ventricle walls of MRL+/+ mice contain protuberances composed primarily of neuroblasts (often marginated by astrocytes) and progenitor cells positive for DCX and BrdU markers (Baker et al., 2006). We confirmed this finding (Fig. 2A) and expanded our analysis to the MRL/lpr substrain and different age groups. Protuberances were not seen at 1 month of age but were more frequent in 4-month-old MRL/lpr mice than in age-matched controls (Substrain × Age interaction: F(1,41) = 4.217, p = .046; Fig. 2C). In some cases, “fusing” of unknown origin was observed between protuberant nests on opposing sides of the ventricular wall (Fig. 2B).

As previously reported (Alexander, Murphy, Roths, and Alexander, 1983; Vogelweid, Johnson, Besch-Williford, Basler, and Walker, 1991; Farrell, Sakic, Szechtman, and Denburg, 1997; James *et al.*, 2006), the choroid plexus (most often in the dorsal 3rd ventricle) of diseased MRL/lpr mice contained numerous cells that stained positive for both Ki67 and BrdU (Fig. 3A, D). These signals were seen in 99% brains from MRL-lpr mice, while no choroids plexus proliferative cells were found in age-matched MRL +/+ controls (Fig. 3B), 1- month-old MRL groups, or 5-month-old C57Bl/6 mice (data not shown). The intraventricular foramen of autoimmune mice was often infiltrated with $CD3^+$ cells, which did not stain for the BrdU marker (Fig. 3C). In addition, $BrdU^+$ cells in the surrounding parenchyma did not stain for NeuN (Fig. 3D). Thus, proliferating cells in the choroid plexus and neighboring regions were neither T-cells, nor $NeuN^+$ neurons.

Periventricular areas

The size of the RMS was assessed from four subsequent sections (Fig. 4A inset). Compared to a continuous projection in the control group, $BrdU^+$ cells in diseased MRL/lpr mice were segregated in small, discontinuous clusters (Fig. 4A, B). The lack of BrdU/NeuN co-labeling

confirmed that the cells in RMS were not mature neurons (Fig. 4C). The spline length of RMS (delineated by $BruU^+$ cells) was significantly smaller in 4-month-old MRL/lpr mice than in age-matched MRL +/+ controls (228.5±8μm vs. 282.5±9.6μm, $|t_{18}|= 4.313$, $p< .001$). Additional analysis confirmed that both $BrdU^+$ and $Ki67^+$ cell areas were smaller in 4-month-old MRL/lpr mice (Fig. 4D), but this was not the case at 1 and 5 months of age due to higher $Ki67^+$ counts in young MRL/lpr mice and comparable group means at 5 months of age, respectively. As expected, the density of $BrdU^+$ cells decreased significantly from 4 to 5 months of age due to cell maturation and differentiation. Moreover, in diseased MRL/lpr mice, a smaller RMS $Ki67^+$ cell area was associated with increased lateral ventricle to brain area ratio for the corresponding sections ($rho_{23}= -0.399$, $p<0.05$). This relationship was not seen in controls, suggesting that altered morphology of RMS accompanies ventricular enlargement. Similarly, a significant positive correlation ($r_{23}= 0.402$, $p<0.05$) between the RMS $Ki67^+$ cell area and the length of the dentate gyrus in diseased MRL/lpr mice suggested that both neurogenic regions were affected by a common pathogenic process.

Subgranular zone (SGZ)

In 4-month-old animals, more FJC^+ cells were detected in the dentate gyrus of MRL/lpr mice than in age-matched controls (Fig. 5). However, this difference was no longer observed at 5 months of age. The measurement of SGZ blade length suggested a smaller DG in MRL/lpr mice which exacerbated from 4 to 5 months of age ($F(1,41) = 4.952$, $p = .032$; Fig. 6A). This was confirmed by assessing the DG area: in 4 month-old MRL-lpr mice = 31652.7±747.1 μm^2 vs. 34566.6±891.5 μm^2 in controls ($|t_{18}|= 2.505$, $p =.022$); in 5 month-old MRL-lpr mice = 28600.8±404.5μm^2 vs. 36153.1±1181.7 μm^2 in controls ($|t_{23}|= 7.013$, $p < .001$). Twenty-four hours after the last BrdU injection (i.e. 4-months old mice), more $BrdU^+$ cells were seen in DG sections from MRL/lpr mice than from MRL +/+ mice ($|t_{18}|= 2.755$, $p = .013$). One month after the last injection however (i.e. 5-months old mice), this trend was inverted ($F(1,41) = 19.487$, $p < .001$; Fig. 6B), suggesting increased cell proliferation at the disease onset, followed by a decreased cell survival in 5 month-old MRL/lpr mice. In addition, assessment of co-localization between BrdU and the neuronal NeuN marker revealed that 24% of cells were double-positive in the 5 moth-old MRL/lpr group, as opposed to 37% in age-matched MRL +/+ mice (Fisher exact test: $p = 0.017$). When cell survival and neuronal differentiation rate were taken into account, it was estimated that 5 month-old MRL +/+ mice had ~3 times more net neurogenesis than diseased MRL/lpr mice ($|t_{23}|= 5.034$, $p < .001$, Figure 6B, Inset). Scarce $Ki67^+$ cells were found along the SGZ, and they did not co-localize with the NeuN marker. Although group means were comparable at 4 months of age (2.7± 0.3 vs. 2.9±0.3, $t_{18} = 0.404$, n.s.), the $Ki67^+$ cell counts (per section) were lower in the 5-month-old MRL-lpr group than in age-matched controls (1.7±0.1 vs. 2. 7±0.2, $t_{18}= 3.995$, $p < .001$). Moreover, in diseased MRL/lpr mice, reduced length of the SGZ was associated with increased lateral ventricle to brain area ratio for sections that encompass the hippocampus ($r_{23} =-0.572$, $p=0.003$, Fig. 6C). No significant correlation between LV:brain area ratio and mean DG length was seen in the control MRL +/+ group ($r_{17} = -0.059$, n.s.). Taken together, the above results suggest that enhanced proliferation at the onset of autoimmune disease is not paralleled by augmented neuronal differentiation along the disease progress. Furthermore, it seems that

the proliferative layer in the dentate gyrus diminishes in parallel with the ventricular enlargement.

Paraventricular nucleus (PVN)

An unexpected observation was the presence of a $Ki67^+$ cell population in the PVN of MRL mice. Few cells were detected in both MRL groups as early as 1 month of age (Fig 7A). However, they were significantly more abundant in 4-month-old MRL/lpr mice than in age-matched controls and 5-month-old, healthy C57 mice (Fig 7B–D). This age-dependent increase in the Ki67 signal (Age: $F(2,47) = 6.184$, $p = .004$; Substrain: $F(2,47) = 4.98$, $p = .03$, Fig. 8A) was associated with increased lateral ventricle to brain area ratio in diseased MRL/lpr mice when sections at the PVN level were considered exclusively ($r_{23} = 0.448$, $p<0.05$, Fig 8B). Further immunohistochemical analysis revealed that the $Ki67^+$ cells did not express the NeuN marker (Fig. 9A) but could also be seen in neighboring, arginine-vasopressin rich regions, such as supraoptic nucleus (SO), supraoptic decussation (SOX) and median eminence (ME) of adult MRL mice (Fig. 9B–D). As shown in Figure 10 and summarized in Table 1, additional cellular markers (BrdU, CD3, FJC, DCX, and GFAP) failed to determine the phenotype of this cell population. Although the cell phenotype and the nature of the underlying process remain unknown, this unique Ki67-associated phenomenon may reflect an important functional alteration that accounts for deficiencies in the neuroendocrine system during SLE.

Discussion

The current study reveals that the onset of chronic autoimmune disease is accompanied by alterations in the two major neurogenic regions. The parallel course of splenomegaly, ventricular enlargement, hindered neuronal differentiation, increased neuronal death and shrinkage of the dentate gyrus suggest that the development of lupus induces neurodegenerative changes that involve impaired proliferative capacity of the brain. The neurobiological nature of increased protuberant nest formation, infiltration of proliferative cells into the choroid plexus, and enhanced Ki67 signal in the PVN requires further study.

The current results build upon prior knowledge of autoimmunity-associated neurodegeneration. An age-dependent increase in ventricle/brain area ratio is consistent with the high incidence of hydrocephalus in the MRL/lpr substrain (Denenberg et al., 1992). Similarly, the increased FJC staining in the SGZ matches the localization of dark, toluidine-stained cells in the dentate gyrus (Ballok et al., 2006). Although infiltration of leukocytes into the choroid plexus has been previously documented (Alexander *et al.*, 1983; Vogelweid *et al.*, 1991; Farrell *et al.*, 1997), the present data expand this finding by identifying proliferative non-T-cells. The formation of protuberances in the SVZ seems to reflect a unique regenerative capacity of peripheral organs (Clark, Clark, and Heber-Katz, 1998; Leferovich, Bedelbaeva, Samulewicz, Zhang, Zwas, Lankford, and Heber-Katz, 2001) and the brain in the MRL strain (Baker et al., 2006). However, it appears that their formation is associated with the disease onset, first in the MRL/lpr substrain and later in aged MRL+/+ mice, who start to show increased production of serum anti-nuclear antibodies (Sakic, Szechtman, Denburg, Carbotte, and Denburg, 1993).

Several pathogenic mechanisms may explain the present results. Given that MRL/lpr brains are deficient in FasR expression (Park, Sakamaki, Tachibana, Yamashima, Yamashita, and Yonehara, 1998), one may assume that the lack of Fas-dependent apoptotic mechanism has consequences on brain development and morphology. In this context, the evidence that programmed cell death is important for the migration of neuroblasts along the RMS (Kim, Kim, Eun, Park, Kim, Kim, Park, Vinsant, Oppenheim, and Sun, 2007) raises the possibility that inherited Fas deficiency disrupts cell migration, accounting for an aberrant shape of the RMS. However, given that increased ventricle/brain area ratio, emergence of protuberances, and SGZ shrinkage occur mainly at the onset of autoimmune disease, this deficiency seems unlikely to account for these effects. Second, neuroinflammation is reported to disrupt neurogenesis (Monje, Toda, and Palmer, 2003) via activated microglia (Ekdahl, Claasen, Bonde, Kokaia, and Lindvall, 2003). Increased microglial activation (Ballok et al., 2006) and increased pro-inflammatory cytokine gene expression in the hippocampus of diseased MRL/lpr mice (Tomita, Holman, and Santoro, 2001) point to the possibility that a local neuroinflammatory process disturbs neurogenesis in the DG. Finally, several studies have shown that systemic and intracerebroventricular administration of brain-reactive antibodies leads to neuronal loss in the hippocampus and behavioral deficits (DeGiorgio *et al.*, 2001; Kowal, DeGiorgio, Nakaoka, Hetherington, Huerta, Diamond, and Volpe, 2004; Huerta, Kowal, DeGiorgio, Volpe, and Diamond, 2006). These studies implied a direct role of autoantibodies in CNS damage during lupus-like disease. However, given the etiological and clinical complexity of CNS-SLE, it is possible that other pathogenic mechanisms contribute to the changes in germinal centers.

More recently, we showed that cells from the C17.2 neural stem cell line and neurospheres from several mouse strains die when incubated with cerebrospinal fluid (CSF) from diseased MRL/lpr mice (Sakic et al., 2005b). Therefore, the pathogenic cascade *in vivo* may include drainage of circulating immune factors (e.g., activated cytotoxic lymphocytes, cytokines and/or autoantibodies) via breached blood-brain barrier into the CSF and diffusion into neighboring tissue, leading to subsequent detrimental effects on proliferative cells. However, the present results suggest a rather complex response to this toxic mechanism. Namely, the analysis of RMS reveals a relatively constant pool of $Ki67^+$ cells during the disease progress in MRL/lpr mice, as opposed to the fluctuation seen in controls (Fig. 4). The surplus in Ki67 cells in 1-month-old MRL/lpr mice may reflect an ongoing reparative response to maternal autoimmune environment that was initiated prior to the formation of a functional blood-brain barrier (Denenberg, Mobraaten, Sherman, Morrison, Schrott, Waters, Rosen, Behan, and Galaburda, 1991; Lee, Huerta, Zhang, Kowal, Bertini, Volpe, and Diamond, 2008). This capacity may remain limited due to sustained cytotoxic effects of CSF on progenitor cells in SVZ at 4 months of age (Romanko, Rola, Fike, Szele, Dizon, Felling, Brazel, and Levison, 2004; Sakic *et al.*, 2005b). Similarly, an excess of $BrdU^+$ cells in the SGZ of 4-month-old MRL/lpr mice might reflect a comparable reparative process that is delayed due to dissimilar exposure to circulating CSF. In particular, while cells in the SVZ are in intimate contact with CSF, proliferating cells in the SGZ are relatively protected by hippocampal parenchyma. If central reparative processes take place in lupus-like disease, the observed shape of RMS is consistent with a widespread neuronal injury (Ballok *et al.*, 2003; Ballok *et al.*, 2006). Therefore, the reduction and discontinuous pattern of the $BrdU^+$ RMS in 4-month-old

MRL/lpr mice may reflect a tangential migration of neuroblasts to repair remote regions, as shown in a model of striatal insult (Yamashita, Ninomiya, Hernandez, Garcia-Verdugo, Sunabori, Sakaguchi, Adachi, Kojima, Hirota, Kawase, Araki, Abe, Okano, and Sawamoto, 2006).

Protuberances in MRL+/+ mice were proposed to represent an enlarged precursor pool associated with an increase in ventricular lumen (Baker et al., 2006). The authors hypothesized that similar observations were to be found in the dentate gyrus. We support this hypothesis by observing even larger ventricles and more $Ki67^+$ cells in young MRL/lpr mice, and increased numbers of $BrdU^+$ cells in SGZ at 4 months of age. The critical question relates to the nature of the increased number of protuberances in autoimmune MRL/lpr mice. As discussed above, the onset of systemic inflammation and autoimmunity appears as the sole factor in accounting for this discrepancy. The CSF plays a role in the migration of neuroblasts (Sawamoto, Wichterle, Gonzalez-Perez, Cholfin, Yamada, Spassky, Murcia, Garcia-Verdugo, Marin, Rubenstein, Tessier-Lavigne, Okano, and varez-Buylla, 2006), with chemorepulsive guidance molecules influencing migration towards the olfactory bulb (Wu, Wong, Chen, Jiang, Dupuis, Wu, and Rao, 1999; Hu, 1999). Taking into consideration the cytotoxic CSF in SLE-like disease, one may hypothesize that the emergence of protuberant nests and their fusing reflect misguided cellular migration from SVZ to RMS. Increased FJC staining and reduced SGZ size in 4-month-old MRL/lpr mice indicate an accelerated neuronal demise in this region at the onset of systemic autoimmunity. The observed spike in $BrdU^+$ cells and subsequent decline in density of $NeuN^+/BrdU^+$ neurons may reflect a compensatory mechanism aimed at increasing proliferation due to widespread loss of young neurons (Romanko et al., 2004).

When the MRL+/+ brain is injured, the lesion sites are characterized by greater cell loss and prolonged cellular proliferation (Hampton, Seitz, Chen, Heber-Katz, and Fawcett, 2004). Therefore, one may wonder whether autoimmunity-induced damage extends cell cycle in the PVN of MRL/lpr mice. The correlation between the $Ki67^+$ cells and the lateral ventricle:brain area ratio suggests that changes in PVN occur in parallel with the emergence of gross brain pathology. It is known that mature neurons actively regulate their post-mitotic state and that if this control fails, they may re-initiate the cell cycle with a predisposition towards “cycle-related neuronal death” (Herrup and Yang, 2007). Therefore, increased expression of cell cycle proteins in at-risk neurons cannot be taken as sole evidence of neurogenesis (Yang, Geldmacher, and Herrup, 2001). The fact that PVN neurons stain for Ki67 (and not BrdU) is consistent with the possibility of cells extending their G1 phase, never reaching DNA-synthesizing S-phase, and ultimately undergoing cellular demise. Another point of interest is that similar $Ki67^+/BrdU^-$ pattern is detected in neighboring neuropeptide-rich regions (such as SO and ME). The magnocellular neurons of SO and PVN project to the posterior pituitary and secrete neuropeptides arginine/vasopressin (AVP) and oxytocin. Similarly, a group of PVN parvocellular neurons co-secrete AVP and CRH into the anterior pituitary by projecting through the ME (Kupfermann, 1991). Consistent with the above, imbalanced AVP/CRH mRNA expression ratio in the PVN (Sakic, Laflamme, Crnic, Szechtman, Denburg, and Rivest, 1999; Shanks, Moore, Perks, and Lightman, 1999) and disturbed activity of the hypothalamus-pituitary adrenal axis are reported in MRL/lpr mice (Hu, Dietrich, Herold, Heinrich, and Wick, 1993; Lechner, Hu, Jafarian-Tehrani, Dietrich,

Schwarz, Herold, Haour, and Wick, 1996; Lechner, Dietrich, Oliveira dos, Wiegers, Schwarz, Harbutz, Herold, and Wick, 2000). The role of $Ki67^{+}/BrdU^{-}$ neurons in the PVN and AVP overexpression may be of particular importance in understanding the etiology of endocrine and behavioral deficits in the MRL model and SLE patients. The nature of leukocyte infiltration into the choroids plexus and brain parenchyma (Alexander *et al.*, 1983; Vogelweid *et al.*, 1991; Farrell *et al.*, 1997; Ma *et al.*, 2006) remains unknown. Although T cells are traditionally considered as a threat to brain tissue (Steinman, Waisman, and Altmann, 1995), a recent notion of “protective autoimmunity” points to the possibility that T cells in the brain promote neurogenesis and learning (Kipnis, Mizrahi, Hauben, Shaked, Shevach, and Schwartz, 2002; Ziv, Ron, Butovsky, Landa, Sudai, Greenberg, Cohen, Kipnis, and Schwartz, 2006). Consistent with this “healing hypothesis”, we could not demonstrate a significant relationship between the magnitude of T cell infiltration and brain pathology (Sakic et al., 2005a).

In summary, the constellation of observations at the behavioral, neuroanatomical, and endocrine levels suggest profound effects of systemic autoimmunity and inflammation on the limbic areas surrounding the ventricular system. This further supports the hypothesis that CSF becomes toxic during disease development, thus compromising the proliferative capacity and viability of nearby cells. Future studies are required to investigate neurotoxic mechanisms of reduced proliferative cell distribution and to characterize molecular targets. The challenge that remains is to identify the immune factors that impair the brain’s repair capacity and induce lupus-associated CNS disorders.

Acknowledgments

We are thankful to Drs. Nicolas Toni, Fred H. Gage, and Jane Foster for constructive comments and John Jepsen for technical assistance. This work was supported by funds from the Canadian Institutes of Health Research.

References

1. Abbott NJ, Mendonca LL, Dolman DE. The blood-brain barrier in systemic lupus erythematosus. Lupus. 2003; 12:908–915. [PubMed: 14714910]
2. Alexander EL, Murphy ED, Roths JB, Alexander GE. Congenic autoimmune murine models of central nervous system disease in connective tissue disorders. Ann Neurol. 1983; 14:242–248. [PubMed: 6625539]
3. Appenzeller S, Costallat LT, Li LM, Cendes F. Magnetic resonance spectroscopy in the evaluation of central nervous system manifestations of systemic lupus erythematosus. Arthritis Rheum. 2006; 55:807–811. [PubMed: 17013841]
4. Baker KL, Daniels SB, Lennington JB, Lardaro T, Czap A, Notti RQ, Cooper O, Isacson O, Frasca S Jr, Conover JC. Neuroblast protuberances in the subventricular zone of the regenerative MRL/MpJ mouse. J Comp Neurol. 2006; 498:747–761. [PubMed: 16927265]
5. Ballok DA, Ma X, Denburg JA, Arsenault L, Sakic B. Ibuprofen fails to prevent brain pathology in a model of neuropsychiatric lupus. J Rheumatol. 2006; 33:2199–2213. [PubMed: 17086606]
6. Ballok DA, Millward JM, Sakic B. Neurodegeneration in autoimmune MRL-lpr mice as revealed by Fluoro Jade B staining. Brain Res. 2003; 964:200–210. [PubMed: 12576180]
7. Bloch DB, Rabkina D, Bloch KD. The cell proliferation-associated protein Ki-67 is a target of autoantibodies in the serum of MRL mice. Lab Invest. 1995; 73:366–371. [PubMed: 7564269]
8. Bosma GP, Middelkoop HA, Rood MJ, Bollen EL, Huizinga TW, van Buchem MA. Association of global brain damage and clinical functioning in neuropsychiatric systemic lupus erythematosus. Arthritis Rheum. 2002; 46:2665–2672. [PubMed: 12384925]

9. Clark LD, Clark RK, Heber-Katz E. A new murine model for mammalian wound repair and regeneration. Clin Immunol Immunopathol. 1998; 88:35–45. [PubMed: 9683548]
10. Danilov AI, Covacu R, Moe MC, Langmoen IA, Johansson CB, Olsson T, Brundin L. Neurogenesis in the adult spinal cord in an experimental model of multiple sclerosis. Eur J Neurosci. 2006; 23:394–400. [PubMed: 16420447]
11. Darsalia V, Heldmann U, Lindvall O, Kokaia Z. Stroke-induced neurogenesis in aged brain. Stroke. 2005; 36:1790–1795. [PubMed: 16002766]
12. DeGiorgio LA, Konstantinov KN, Lee SC, Hardin JA, Volpe BT, Diamond B. A subset of lupus anti-DNA antibodies cross-reacts with the NR2 glutamate receptor in systemic lupus erythematosus. Nat Med. 2001; 7:1189–1193. [PubMed: 11689882]
13. Denenberg VH, Mobraaten LE, Sherman GF, Morrison L, Schrott LM, Waters NS, Rosen GD, Behan PO, Galaburda AM. Effects of the autoimmune uterine/maternal environment upon cortical ectopias, behavior and autoimmunity. Brain Res. 1991; 563:114–122. [PubMed: 1786524]
14. Denenberg VH, Sherman GF, Rosen GD, Morrison L, Behan PO, Galaburda AM. A behavior profile of the MRL/Mp lpr/lpr mouse and its association with hydrocephalus. Brain Behav Immun. 1992; 6:40–49. [PubMed: 1571603]
15. Ekdahl CT, Claasen JH, Bonde S, Kokaia Z, Lindvall O. Inflammation is detrimental for neurogenesis in adult brain. Proc Natl Acad Sci U S A. 2003; 100:13632–13637. [PubMed: 14581618]
16. Farrell M, Sakic B, Szechtman H, Denburg JA. Effect of cyclophosphamide on leucocytic infiltration in the brain of MRL/lpr mice. Lupus. 1997; 6:268–274. [PubMed: 9104735]
17. Hampton DW, Seitz A, Chen P, Heber-Katz E, Fawcett JW. Altered CNS response to injury in the MRL/MpJ mouse. Neuroscience. 2004; 127:821–832. [PubMed: 15312895]
18. Handa R, Sahota P, Kumar M, Jagannathan NR, Bal CS, Gulati M, Tripathi BM, Wali JP. In vivo proton magnetic resonance spectroscopy (MRS) and single photon emission computerized tomography (SPECT) in systemic lupus erythematosus (SLE). Magn Reson Imaging. 2003; 21:1033–1037. [PubMed: 14684208]
19. Herrup K, Yang Y. Cell cycle regulation in the postmitotic neuron: oxymoron or new biology? Nat. Rev Neurosci. 2007; 8:368–378.
20. Hu H. Chemorepulsion of neuronal migration by Slit2 in the developing mammalian forebrain. Neuron. 1999; 23:703–711. [PubMed: 10482237]
21. Hu Y, Dietrich H, Herold M, Heinrich PC, Wick G. Disturbed immuno-endocrine communication via the hypothalamo- pituitary-adrenal axis in autoimmune disease. Int Arch Allergy Immunol. 1993; 102:232–241. [PubMed: 8219776]
22. Huerta PT, Kowal C, DeGiorgio LA, Volpe BT, Diamond B. Immunity and behavior: Antibodies alter emotion. Proc Natl Acad Sci U S A. 2006; 103:678–683. [PubMed: 16407105]
23. James WG, Hutchinson P, Bullard DC, Hickey MJ. Cerebral leucocyte infiltration in lupus-prone MRL/MpJ-fas lpr mice--roles of intercellular adhesion molecule-1 and P-selectin. Clin Exp Immunol. 2006; 144:299–308. [PubMed: 16634804]
24. Jennings JE, Sundgren PC, Attwood J, McCune J, Maly P. Value of MRI of the brain in patients with systemic lupus erythematosus and neurologic disturbance. Neuroradiology. 2004; 46:15–21. [PubMed: 14648006]
25. Kempermann G, Kuhn HG, Gage FH. Genetic influence on neurogenesis in the dentate gyrus of adult mice. Proc Natl Acad Sci U S A. 1997; 94:10409–10414. [PubMed: 9294224]
26. Kim WR, Kim Y, Eun B, Park OH, Kim H, Kim K, Park CH, Vinsant S, Oppenheim RW, Sun W. Impaired migration in the rostral migratory stream but spared olfactory function after the elimination of programmed cell death in Bax knockout mice. J Neurosci. 2007; 27:14392–14403. [PubMed: 18160647]
27. Kipnis J, Mizrahi T, Hauben E, Shaked I, Shevach E, Schwartz M. Neuroprotective autoimmunity: naturally occurring CD4+CD25+ regulatory T cells suppress the ability to withstand injury to the central nervous system. Proc Natl Acad Sci U S A. 2002; 99:15620–15625. [PubMed: 12429857]
28. Kowal C, DeGiorgio LA, Nakaoka T, Hetherington H, Huerta PT, Diamond B, Volpe BT. Cognition and immunity; antibody impairs memory. Immunity. 2004; 21:179–188. [PubMed: 15308099]

29. Kozora E, West SG, Kotzin BL, Julian L, Porter S, Bigler E. Magnetic resonance imaging abnormalities and cognitive deficits in systemic lupus erythematosus patients without overt central nervous system disease. Arthritis Rheum. 1998; 41:41–47. [PubMed: 9433868]
30. Kupfermann, I. Hypothalamus and Limbic System: Peptidergic Neurons, Homeostasis, and Emotional Behavior. In: Kandel, ER.Schwartz, JH., Jessell, TM., editors. Principles of Neural Science. Appleton & Lange; Connecticut: 1991. p. 735-749.
31. Lechner O, Dietrich H, Oliveira dos SA, Wiegers GJ, Schwarz S, Harbutz M, Herold M, Wick G. Altered circadian rhythms of the stress hormone and melatonin response in lupus-prone MRL/MP-fas(Ipr) mice. J Autoimmun. 2000; 14:325–333. [PubMed: 10882059]
32. Lechner O, Hu Y, Jafarian-Tehrani M, Dietrich H, Schwarz S, Herold M, Haour F, Wick G. Disturbed immunoendocrine communication via the hypothalamo-pituitary-adrenal axis in murine lupus. Brain Behav Immun. 1996; 10:337–350. [PubMed: 9045749]
33. Lee JY, Huerta PT, Zhang J, Kowal C, Bertini E, Volpe BT, Diamond B. Neurotoxic autoantibodies mediate congenital cortical impairment of offspring in maternal lupus. Nat Med. 2008
34. Leferovich JM, Bedelbaeva K, Samulewicz S, Zhang XM, Zwas D, Lankford EB, Heber-Katz E. Heart regeneration in adult MRL mice. Proc Natl Acad Sci U S A. 2001; 98:9830–9835. [PubMed: 11493713]
35. Ma X, Foster J, Sakic B. Distribution and prevalence of leukocyte phenotypes in brains of lupus-prone mice. J Neuroimmunol. 2006; 179:26–36. [PubMed: 16904195]
36. Maric D, Millward JM, Ballok DA, Szechtman H, Barker JL, Denburg JA, Sakic B. Neurotoxic properties of cerebrospinal fluid from behaviorally impaired autoimmune mice. Brain Res. 2001; 920:183–193. [PubMed: 11716824]
37. Martino G, Pluchino S. The therapeutic potential of neural stem cells. Nat Rev Neurosci. 2006; 7:395–406. [PubMed: 16760919]
38. Monje ML, Toda H, Palmer TD. Inflammatory blockade restores adult hippocampal neurogenesis. Science. 2003; 302:1760–1765. [PubMed: 14615545]
39. Park C, Sakamaki K, Tachibana O, Yamashima T, Yamashita J, Yonehara S. Expression of Fas antigen in the normal mouse brain. Biochem Biophys Res Commun. 1998; 252:623–628. [PubMed: 9837756]
40. Romanko MJ, Rola R, Fike JR, Szele FG, Dizon ML, Felling RJ, Brazel CY, Levison SW. Roles of the mammalian subventricular zone in cell replacement after brain injury. Prog Neurobiol. 2004; 74:77–99. [PubMed: 15518954]
41. Sakic B, Hanna SE, Millward JM. Behavioral heterogeneity in an animal model of neuropsychiatric lupus. Biol Psychiatry. 2005a; 57:679–687. [PubMed: 15780857]
42. Sakic B, Kirkham DL, Ballok DA, Mwanjewe J, Fearon IM, Macri J, Yu G, Sidor MM, Denburg JA, Szechtman H, Lau J, Ball AK, Doering LC. Proliferating brain cells are a target of neurotoxic CSF in systemic autoimmune disease. J Neuroimmunol. 2005b; 169:68–85. [PubMed: 16198428]
43. Sakic B, Laflamme N, Crnic LS, Szechtman H, Denburg JA, Rivest S. Reduced corticotropin-releasing factor and enhanced vasopressin gene expression in brains of mice with autoimmunity-induced behavioral dysfunction. J Neuroimmunol. 1999; 96:80–91. [PubMed: 10227427]
44. Sakic B, Maric I, Koeberle PD, Millward JM, Szechtman H, Maric D, Denburg JA. Increased TUNEL-staining in brains of autoimmune Fas-deficient mice. J Neuroimmunol. 2000; 104:147–154. [PubMed: 10713354]
45. Sakic B, Szechtman H, Denburg JA, Gorny G, Kolb B, Whishaw IQ. Progressive atrophy of pyramidal neuron dendrites in autoimmune MRL-lpr mice. J Neuroimmunol. 1998; 87:162–170. [PubMed: 9670858]
46. Sakic B, Szechtman H, Denburg SD, Carbotte RM, Denburg JA. Spatial learning during the course of autoimmune disease in MRL mice. Behav Brain Res. 1993; 54:57–66. [PubMed: 8504012]
47. Sakic B, Szechtman H, Talangbayan H, Denburg SD, Carbotte RM, Denburg JA. Disturbed emotionality in autoimmune MRL-lpr mice. Physiol Behav. 1994; 56:609–617. [PubMed: 7972416]
48. Sawamoto K, Wichterle H, Gonzalez-Perez O, Cholfin JA, Yamada M, Spassky N, Murcia NS, Garcia-Verdugo JM, Marin O, Rubenstein JL, Tessier-Lavigne M, Okano H, varez-Buylla A. New

neurons follow the flow of cerebrospinal fluid in the adult brain. Science. 2006; 311:629–632. [PubMed: 16410488]

49. Schmued LC, Stowers CC, Scallet AC, Xu L. Fluoro-Jade C results in ultra high resolution and contrast labeling of degenerating neurons. Brain Res. 2005; 1035:24–31. [PubMed: 15713273]
50. Scholzen T, Gerdes J. The Ki-67 protein: from the known and the unknown. J Cell Physiol. 2000; 182:311–322. [PubMed: 10653597]
51. Shanks N, Moore PM, Perks P, Lightman SL. Alterations in hypothalamic-pituitary-adrenal function correlated with the onset of murine SLE in MRL +/+ and lpr/lpr mice. Brain Behav Immun. 1999; 13:348–360. [PubMed: 10600221]
52. Sibbitt WL, Haseler LJ, Griffey RH, Hart BL, Sibbitt RR, Matwiyoff NA. Analysis of cerebral structural changes in systemic lupus erythematosus by proton MR spectroscopy. AJNR Am J Neuroradiol. 1994; 15:923–928. [PubMed: 8059662]
53. Steinman L, Waisman A, Altmann D. Major T-cell responses in multiple sclerosis. Mol Med Today. 1995; 1:79–83. [PubMed: 17607899]
54. Theofilopoulos, AN. Murine models of lupus. In: Lahita, RG., editor. Systemic lupus erythematosus. Churchill Livingstone; New York: 1992. p. 121-194.
55. Thuret S, Toni N, Aigner S, Yeo GW, Gage FH. Hippocampus-dependent learning is associated with adult neurogenesis in MRL/MpJ mice. Hippocampus. 2009 (Epub ahead of print).
56. Tomita M, Holman BJ, Santoro TJ. Aberrant cytokine gene expression in the hippocampus in murine systemic lupus erythematosus. Neurosci Lett. 2001; 302:129–132. [PubMed: 11290404]
57. Vogelweid CM, Johnson GC, Besch-Williford CL, Basler J, Walker SE. Inflammatory central nervous system disease in lupus-prone MRL/lpr mice: comparative histologic and immunohistochemical findings. J Neuroimmunol. 1991; 35:89–99. [PubMed: 1955574]
58. Watanabe-Fukunaga R, Brannan CI, Copeland NG, Jenkins NA, Nagata S. Lymphoproliferation disorder in mice explained by defects in Fas antigen that mediates apoptosis. Nature. 1992; 356:314–317. [PubMed: 1372394]
59. Waterloo K, Omdal R, Jacobsen EA, Klow NE, Husby G, Torbergsen T, Mellgren SI. Cerebral computed tomography and electroencephalography compared with neuropsychological findings in systemic lupus erythematosus. J Neurol. 1999; 246:706–711. [PubMed: 10460449]
60. Wu W, Wong K, Chen J, Jiang Z, Dupuis S, Wu JY, Rao Y. Directional guidance of neuronal migration in the olfactory system by the protein Slit. Nature. 1999; 400:331–336. [PubMed: 10432110]
61. Yamashita T, Ninomiya M, Hernandez AP, Garcia-Verdugo JM, Sunabori T, Sakaguchi M, Adachi K, Kojima T, Hirota Y, Kawase T, Araki N, Abe K, Okano H, Sawamoto K. Subventricular zone-derived neuroblasts migrate and differentiate into mature neurons in the post-stroke adult striatum. J Neurosci. 2006; 26:6627–6636. [PubMed: 16775151]
62. Yang Y, Geldmacher DS, Herrup K. DNA replication precedes neuronal cell death in Alzheimer's disease. J Neurosci. 2001; 21:2661–2668. [PubMed: 11306619]
63. Ziv Y, Ron N, Butovsky O, Landa G, Sudai E, Greenberg N, Cohen H, Kipnis J, Schwartz M. Immune cells contribute to the maintenance of neurogenesis and spatial learning abilities in adulthood. Nat Neurosci. 2006; 9:268–275. [PubMed: 16415867]

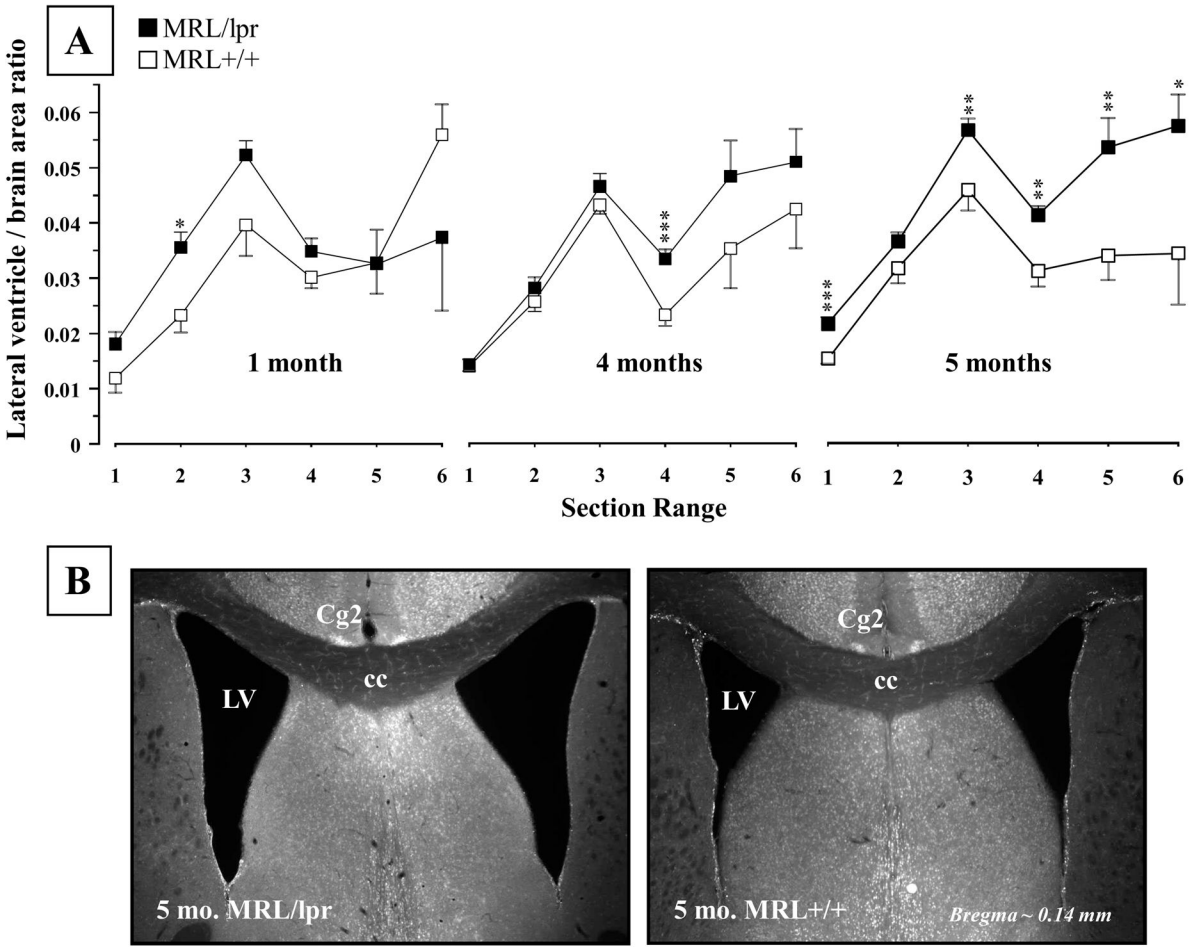

Figure 1.

Mean lateral ventricle to brain area ratio at different ages. (A) In comparison to MRL +/+ controls, a significant increase in ratio was noted in the diseased 5-month-old MRL/lpr group. In addition, occasional enlargement in specific sections was seen at younger ages when T-test was applied (indicated by asterixes). (B) Representative low-power images illustrating enlarged and irregularly shaped lateral ventricles in a MRL/lpr mouse. *Section locations*: 1 = 1.42 to 0.74 mm, 2 = 0.62 to 0.14 mm, 3 = 0.02 to −0.70 mm, 4 = −0.82 to −1.34 mm, 5 = −1.58 to −2.18 mm, 6 = −2.30 to −2.80 mm, relative to Bregma. *Abbreviations*: **Cg2**, cingulate cortex area 2; **cc**, corpus callosum; **LV**, lateral ventricle.

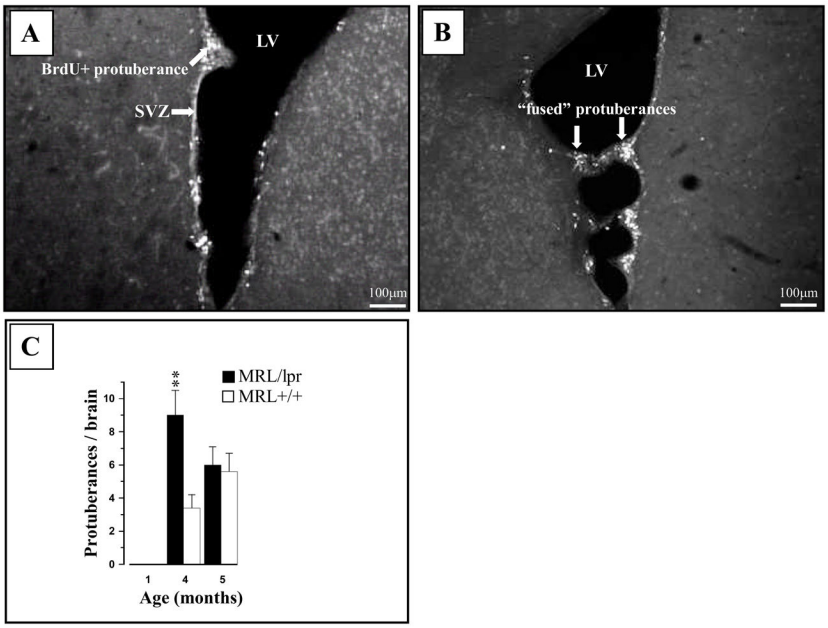

Figure 2.

Representative photos of ventricular protuberances in the 4-month-old MRL brain. (A) The $BrdU^+$ protuberances were commonly seen in the wall of lateral ventricles from both MRL/lpr and MRL +/+ mice (not shown). (B) In some cases, opposing protuberances appeared "fused" (interconnected) by large processes. (C) Protuberances were absent in young mice and more frequent at the onset of disease in MRL/lpr mice.

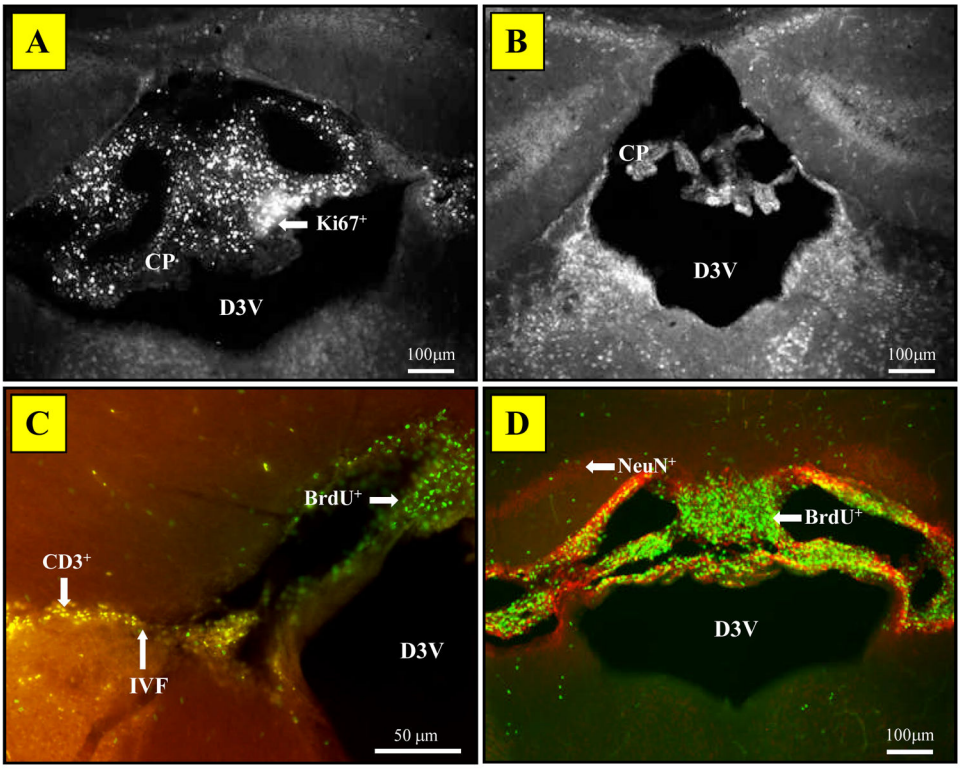

Figure 3.

Representative images of the choroid plexus (CP) in the third ventricle stained with fluorescent markers. (A) The CP abundant with $Ki67^+$ cells in diseased MRL/lpr mice. (B) A lack of proliferating cells in the CP of MRL +/+ mice. (C) Lack of co-localization between $BrdU^+$ and $CD3^+$ cells in CP and adjacent brain parenchyma in MRL/lpr brains. (D) Lack of co-localization for the $BrdU^+$ and $NeuN^+$ cells at the hippocampal level. The above observations suggest that proliferative cells are neither T-lymphocytes nor neurons. *Abbreviations*: **D3V**, dorsal third ventricle; **IVF**, interventricular foramen.

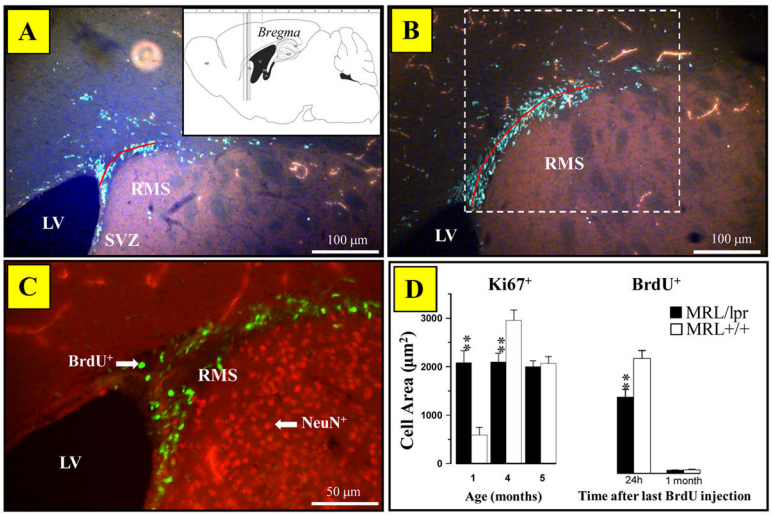

Figure 4.

The assessment of proliferation in RMS. (A) Representative image illustrating reduced spline length (red line), i.e. diameter of RMS and patchy accumulation of $BrdU^+$ cells in a diseased MRL/lpr brain (*Inset*: location of brain sections used in quantitative analysis). (B) Elongated and continuous projection of $BrdU^+$ cells in an age-matched MRL +/+ mouse. Dashed border shows approximate location of the signal area counting frame. (C) Lack of BrdU and NeuN co-localization, confirming that the migrating cells are not adult neurons. (D) Dissimilar patterns of $Ki67^+$ expression between MRL/lpr and MRL +/+ mice during first five months of life. The density of $Ki67^+$cells remain relatively constant in MRL/lpr mice, whereas significant fluctuations occur in the MRL +/+ group. Consistent with the notion of impaired capacity of the brain at the onset of systemic autoimmunity, 4-month-old MRL/lpr mice showed decreased numbers of $Ki67^+$ and $BrdU^+$ cells (24h after last injection) in comparison to age-matched controls. *Abbreviations*: **RMS**, rostral migratory stream; **LV**, lateral ventricle; **SVZ**, subventricular zone of the lateral ventricle.

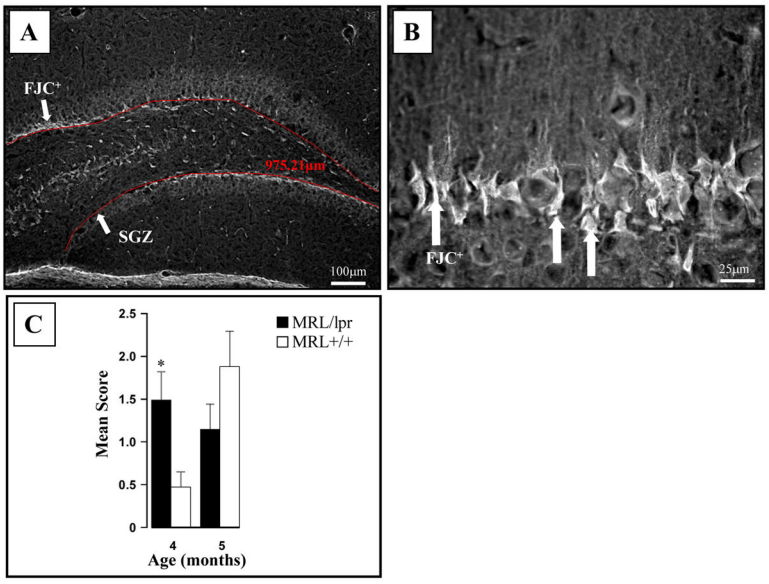

Figure 5.

FJC staining in the hippocampus. (A). A representative photo showing FJC$^+$ neurons along the continuous SGZ of the dentate gyrus of MRL/lpr mouse and automated length assessment by AxioVision 4.6 (in red). (B) Higher magnification confirmed the selective involvement of the SGZ. (C) Four-month-old autoimmune mice showed increased FJC staining, followed by a similar increase in older MRL +/+ mice.

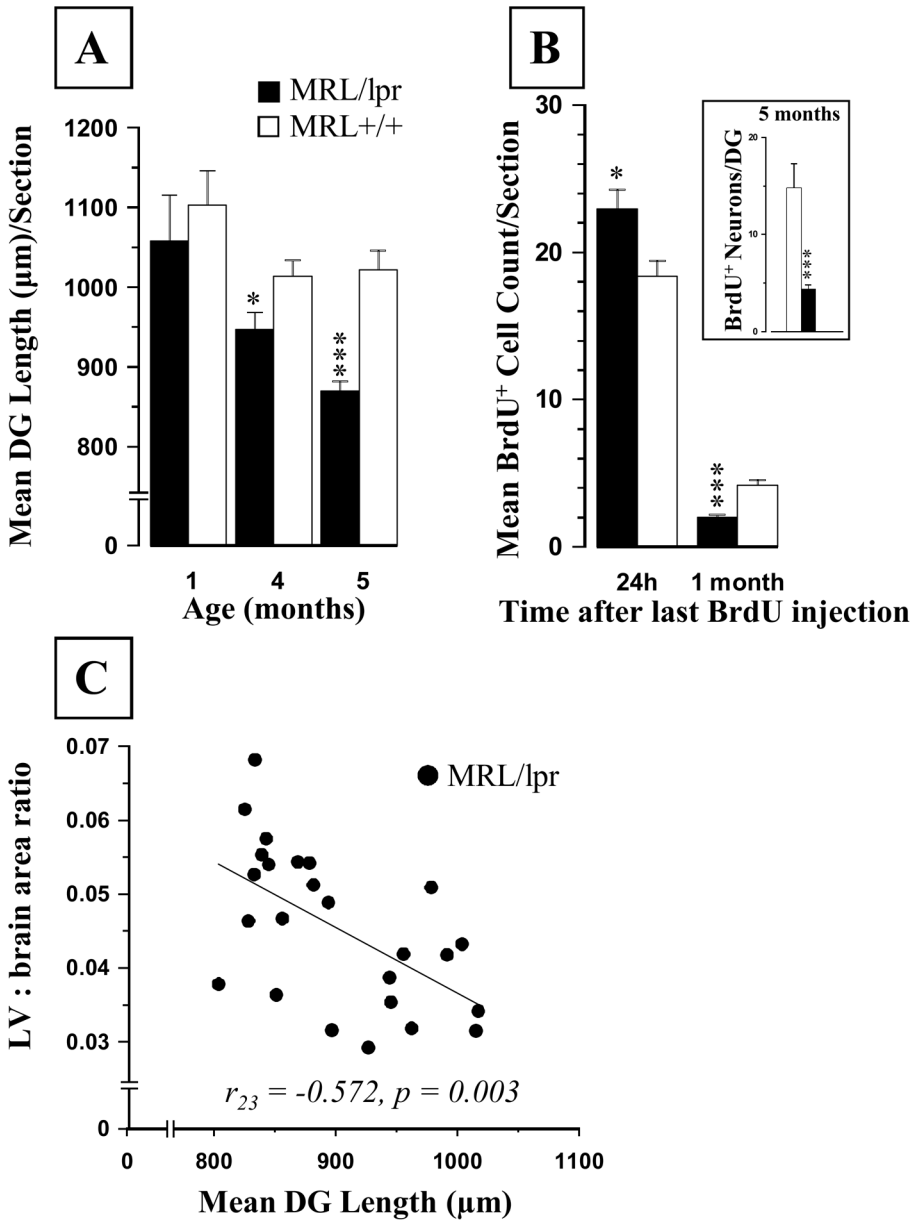

Figure 6.

Age-dependent changes in the dentate gyrus (DG). (A) The length of the SGZ declined continuously with age, but this decrease was steeper in diseased MRL/lpr mice. (B) The $BrdU^+$ cell counts in the SGZ of 4-month-old MRL/lpr mice were higher but showed a sharper decline one month later in comparison to age-matched MRL +/+ controls. (*Inset:* The sum of $NeuN^+$ cells relative to the total number of $BrdU^+$ cells in DG region from −1.58 to −2.54 mm from Bregma). (C) The increased lateral ventricle to brain area ratio at the level of hippocampus was associated with smaller SGZ length, suggesting that ventricular enlargement is accompanied by reductions in this proliferative zone (* $p \leq .05$, *** $p < .001$).

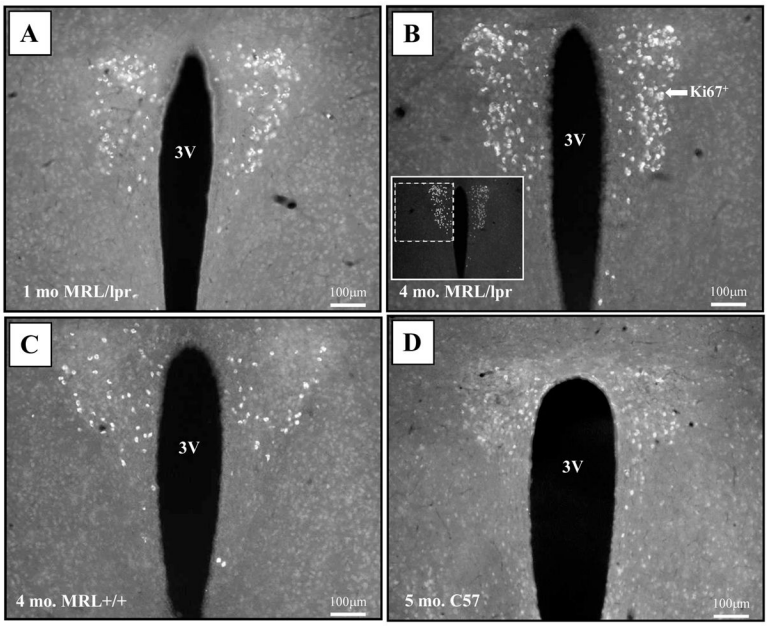

Figure 7.

Population of Ki67^{+}cells in the paraventricular nucleus (PVN). (A) The Ki67^{+} cells were present in both 1-month-old MRL/lpr and MRL +/+ mice (photo not shown). (B) This signal intensified at the onset of autoimmune disease in 4-month-old MRL/lpr mice. (C) A detectable but less abundant signal was present in age-matched MRL +/+ controls. (D) A faint signal, undetectable to the imaging software, was also seen in 5-month-old healthy C57 controls. *Abbreviations*: **3V**, ventral third ventricle

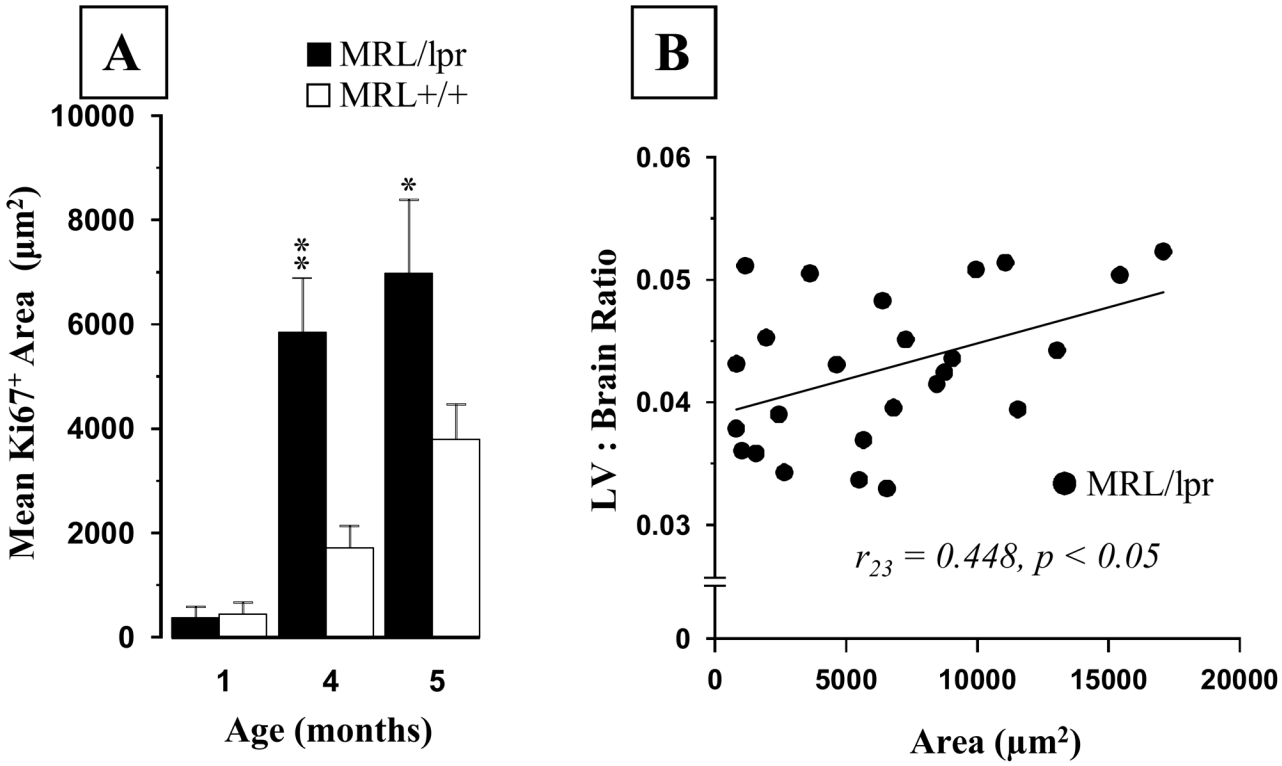

Figure 8.

Quantification of the Ki67 signal in the PVN. (A) The area of Ki67 signal was comparable before the onset of autoimmune disease in MRL/lpr mice. However, it became significantly larger with increasing age. (B) The increased lateral ventricle to brain area ratio at the level of PVN sections was positively associated with the size of $Ki67^+$ area, suggesting that ventricular enlargement was accompanied by enhanced expression of this unexpected signal.

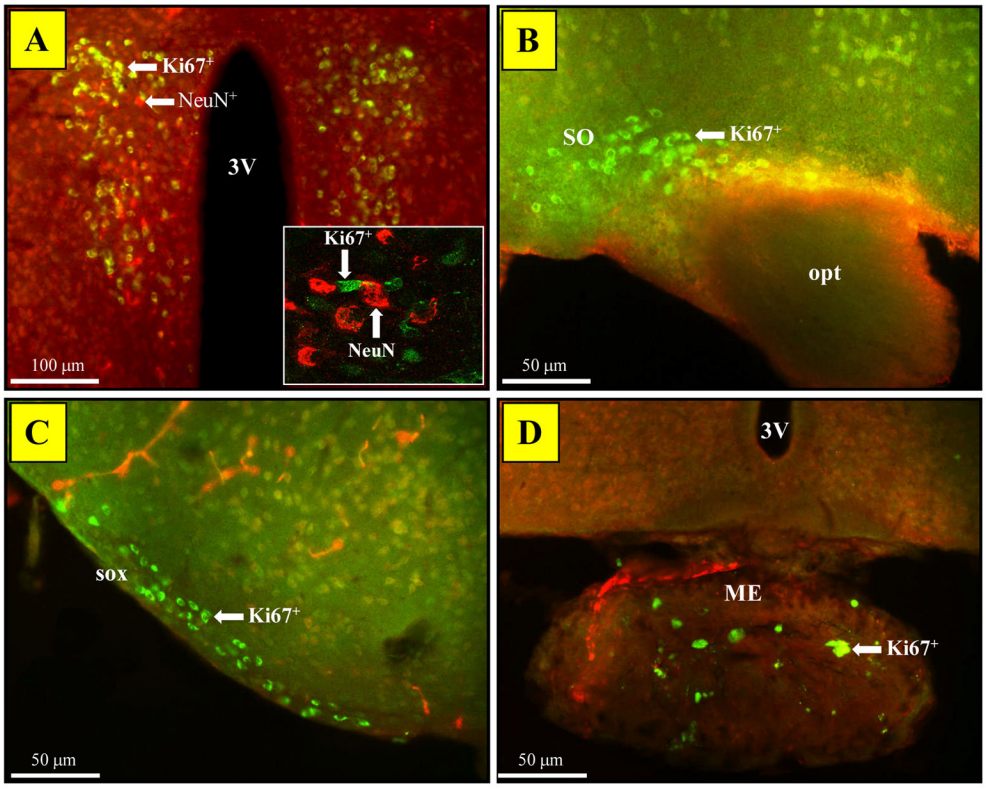

Figure 9.

Ki67 signal distribution in PVN-neighboring regions. (A) Standard immunofluorescence revealed a lack of co-localization between Ki67 and NeuN signals in the PVN (*Inset:* Confocal microscopy confirmed adjacent cells distinctly labeled with Ki67 or NeuN). (B) The Ki67 staining identified cells in the supraoptic nucleus of both MRL/lpr (shown) and MRL +/+ mice at all ages. (C) Similarly, supraoptic decussation and (D) median eminence contained sparse, but clearly labeled $Ki67^{+}/NeuN^{-}$ cells. *Abbreviations*: **3V**, ventral third ventricle; **SO**, supraoptic nucleus; **opt**, optic tract; **sox**, supraoptic decussation; **ME,** median eminence.

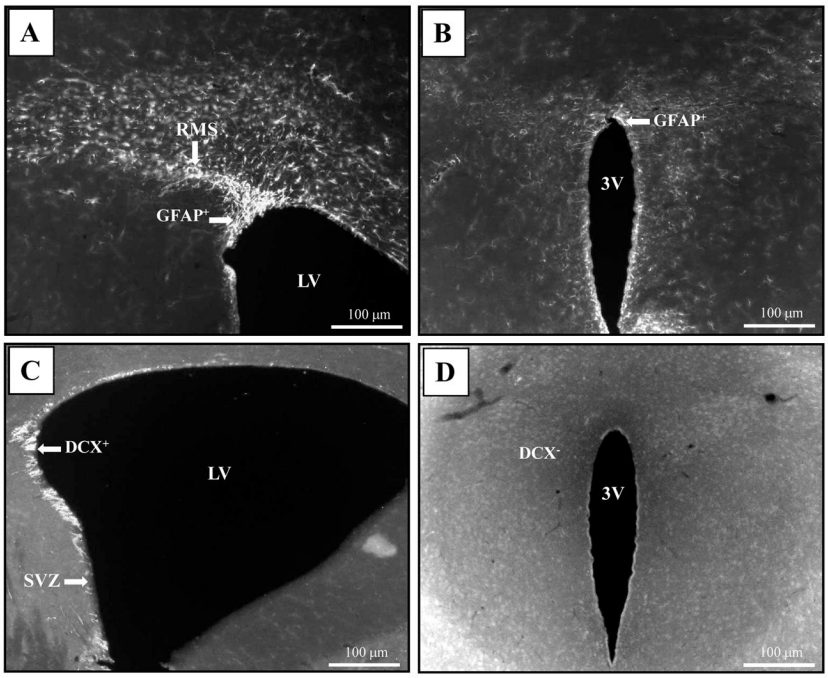

Figure 10.

Representative photos of GFAP and DCX signal distributions in SVZ and PVN regions of an MRL/lpr brain. (A) $GFAP^+$ cells projecting from the lateral ventricle along the RMS. (B) The same section revealed a rim pattern staining around the third ventricle, but no signal was detected in the PVN. (C) As expected, the SVZ region showed a population of DCX^+ cells. (D) Conversely, the same brain section demonstrated a lack of the same signal in the PVN. *Abbreviations*: **3V**, ventral third ventricle; **LV**, lateral ventricle; **RMS**, rostral migratory stream.

Table 1

The summary of immunohistochemical findings in diseased MRL/lpr mice. The Ki67 and BrdU markers confirm cell proliferation in major neurogenic regions. However, proliferating cells are also found in protuberances and within cells infiltrating the choroid plexsus. Unexpected $Ki67^{+}$ signal in the PVN and lack of co-labeling with other proliferative markers suggest a unique process in this important neuroendocrine region.

	Ki67	BrdU	NeuN	CD3	FJC	DCX	GFAP
SVZ	+	+	−	−	+	+	+
SGZ	+	+	−	−	+	+	+
PVN	+	−	−	−	−	−	−
Protuberances	+	+	−	−	−	+?	−
Choroid Plexus	+	+	−	+	−	−	−